SynCAM1, a Synaptic Adhesion Molecule, Is Expressed in Astrocytes and Contributes to erbB4 Receptor-Mediated Control of Female Sexual Development

Ursula S. Sandau,* Alison E. Mungenast,* Zefora Alderman, S. Pablo Sardi, Adam I. Fogel, Bethany Taylor, Anne-Simone Parent, Thomas Biederer, Gabriel Corfas, and Sergio R. Ojeda

Division of Neuroscience (U.S.S., A.E.M., Z.A., A.-S.P., S.R.O.), Oregon National Primate Research Center/ Oregon Health and Science University, Beaverton, Oregon 97006; F. M. Kirby Neurobiology Program (S.P.S., B.T., G.C.), Children's Hospital, Harvard Medical School, Boston, Massachusetts 02115; and Department of Molecular Biophysics and Biochemistry (A.I.F., T.B.), Yale University, New Haven, Connecticut 06520

Female sexual maturation requires erythroblastosis B (erbB)4 signaling in hypothalamic astrocytes; however, the mechanisms by which erbB4 contributes to this process are incompletely understood. Here we show that SynCAM1, a synaptic adhesion molecule with signaling capabilities, is not only expressed highly in neurons, but also in hypothalamic astrocytes and is functionally associated with erbB4 receptor activity. Whereas SynCAM1 expression is diminished in astrocytes with impaired erbB4 signaling, ligand-dependent activation of astroglial erbB4 receptors results in rapid association of erbB4 with SynCAM1 and activation of SynCAM1 gene transcription. To determine whether astrocytic SynCAM1-dependent intracellular signaling is required for normal female reproductive function, we generated transgenic mice that express in an astrocyte-specific manner a dominant-negative form of SynCAM1 lacking the intracellular domain. The mutant protein was correctly targeted to the cell membrane and was functionally viable as shown by its ability to block intracellular calcium/calmodulin-dependent serine protein kinase redistribution, a major SynCAM1-mediated event. Dominant-negative-SynCAM1 female mice had a delayed onset of puberty, disrupted estrous cyclicity, and reduced fecundity. These deficits were associated with a reduced capacity of neuregulin-dependent erbB4 receptor activation to elicit prostaglandin E2 release from astrocytes and GnRH release from the hypothalamus. We conclude that one of the mechanisms underlying erbB4 receptor-mediated facilitation of glial-neuronal interactions in the neuroendocrine brain involves SynCAM1-dependent signaling and that this interaction is required for normal female reproductive function. (*Endocrinology* 152: 2364–2376, 2011)

The erythroblastosis (erbB) family of tyrosine kinase receptors and their respective ligands regulate a variety of developmental processes and mature cellular functions in different tissues (1). In the nervous system, erbB receptors not only contribute to the control of neurogenesis and transsynaptic communication but also play a central role in the regulation of glial biology and development (2, 3). In the case of astrocytes, it was recently shown that neu-regulin (NRG)-1-dependent activation of erbB receptors regulates the timing of astrogenesis in brain (4). Yet little is known about the contribution of NRG-erbB signaling to other aspects of astrocyte biology.

An area in which we are beginning to better understand the mechanisms by which NRG1-erbB signaling regulates neuron-astrocyte interactions is the mammalian hypothalamus. Hypothalamic astrocytes express erbB2 and erbB4 receptors but are devoid of erbB3 receptors (5). Ligand-dependent activation of an astroglial erbB4/2 complex sets in motion a signaling cascade that results in prostaglandin E_2 (PGE_2) production (5). PGE_2 then stimulates secretion of GnRH, the neuropeptide controlling sexual development, from hypothalamic neurons (6). In mice expressing a dominant-negative (DN) erbB4 receptor in hypothalamic astrocytes [glial fibrillary acidic protein (GFAP)-DNerbB4] these events are inhibited, with GFAP-DNerbB4 female mice having delayed sexual maturation and diminished reproductive capacity (7). These deficiencies are associated with reduced PGE_2 formation and impaired capacity of the mutant astrocytes to elicit GnRH release in response to NRG1 stimulation.

To identify the gene products affected by this astrocytic-specific disruption in erbB signaling we used isotope-coded affinity tags (ICAT) (8), a proteomics approach that identifies and quantifies individual components of highly heterogeneous protein mixtures (9, 10), such as those found in the nervous system. By comparing the hypothalamic proteome of wild-type (WT) mice to GFAP-DNerbB4 mice, we identified synaptic cell adhesion molecule 1 [SynCAM1; also named tumor suppressor of lung cancer-1 (Tslc1); and Nectin-like protein 2], a synaptic adhesion molecule with signaling capabilities encoded by the *CADM1* gene (11), as a protein affected by the loss of astrocytic erbB4 function. In the companion paper, we establish that SynCAM1 is a mediator of adhesion between hypothalamic astrocytes and GnRH neurons (12). Here we show that SynCAM1 is expressed in hypothalamic astrocytes and this expression is regulated by erbB4 signaling. Our results show that SynCAM1, as a signaling molecule, uses its intracellular domain to mediate erbB4-dependent activation of astrocyte-to-GnRH neuron communication, thereby facilitating the timely initiation of adult female reproductive function.

Materials and Methods

Animals

GFAP-DNerbB4, DN SynCAM1 and WT FvB mice were used in accordance with National Institutes of Health guidelines for the Care and Use of Laboratory Animals. All experimental protocols were approved by the Animal Care and Use Committee of the Oregon National Primate Research Center.

ICAT labeling

A region rostral to the hypothalamus containing the diagonal band of Broca and preoptic area (for simplicity referred to as the POA) was dissected from four GFAP-DNerbB4 and four WT FvB immature (d 28) female mice and rapidly frozen on dry ice. The tissue was then transported to the Institute for Systems Biology in Seattle, WA, in which the proteins were extracted with mammalian protein extraction reagent following the manufacturer's protocol (Pierce, Rockford, IL). The samples were spun to pellet-insoluble material and then dried down to 100 μl. The protein content of each sample was determined with the Pierce BCA reagent. Four hundred microliters of labeling buffer (0.05% sodium dodecyl sulfate; 200 mM Tris, pH 8.3; 5 mM EDTA; 6 M urea) were added to each sample. The proteins were reduced with 5 mM Tris, 2-carboxyethylphosphine. Then 535 nmol of the ICAT reagent were added to each sample (9). Proteins from the POA of WT mice were labeled with the light ICAT reagent, and the proteins from the POA of GFAP-DNerbB4 mice were labeled with the heavy ICAT form. Because this form contains eight deuteriums, it is 8 Da heavier than the light reagent that contains no deuterium (8). The labeling reaction was incubated for 90 min at room temperature. An aliquot of each sample was run on a SDS-PAGE gel to check for labeling, indicated by a small shift in the size of the Coomassie-stained protein bands. The ICAT reaction was then quenched with an excess of dithiothreitol (13), and the proteins were digested overnight at 37 C with trypsin (1:50, wt/wt). Complete digestion was verified via SDS-PAGE and Coomassie staining. The resultant peptides were subjected to separation on a strong-ion exchange column and ICAT-bound peptides were isolated using an avidin-affinity column (8, 13). These purified peptides were lyophilized and processed as described below.

Mass spectrometry

Peptide mixtures were analyzed by electrospray ionization tandem mass spectrometry coupled to capillary liquid chromatography (μLC-MS/MS) (8, 9). The procedure was performed in the proteomics core facility at the Institute for Systems Biology, and the data gathered were retrieved on-line. The lyophilized peptides were solubilized in 50 μl of an aqueous solution of 0.4% acetic acid and 0.005% heptafluorobutyric acid. Approximately 2 μl of this solution was pressure bomb loaded onto a 75 μm inner diameter reverse-phase capillary column packed with 10 cm of Magic C18 resin (Michrom Bioresources, Auburn, CA). The peptides were subsequently eluted off the column using a linear solvent gradient of increasing acetonitrile concentration and ionized using electrospray ionization with a liquid chromatography set-up, as described (14). The ionized liquid chromatography stream was analyzed by tandem mass spectrometry on a LCQ-Classic (Thermofinnigan, San Jose, CA).

Using this μLC-MS/MS system, the ICAT-labeled peptide pairs coeluting from the C18 column were automatically quantified by measuring their ratios before they entered the mass spectrometer. Alternative scans were also automatically selected for mass spectrometry fragmentation via collision-induced dissociation (CID). Amino acid sequence assignments were then generated from the CID analysis by searching the mass spectrometer data files against a mouse peptide/protein database using the SEQUEST algorithm (15). The SEQUEST-generated lists

TABLE 1.   Primers used for conventional PCR and real-time PCR

		Conventional PCR primers			
Gene name	**Accession no.**	**Sense primer**	**Position**	**Antisense primer**	**Position**
SynCAM1 promoter	NT_033899	tatttttattagagacggagtttc	18,939,510-487	gcggacagctaatgagatg	18,937,656-578
DN SynCAM1	AF539424	agatctaggcgtgtacggtgggaggtcta	122–145	gtcgacgcaaaatagcggcccagaatgat	1405–1428
DN SynCAM1 genotyping	AF539424 and U55762	cctcccacaacaaccaccaccact	1140–1163	gccctcgccggacacgctgaac	759–780
CASK	NM_022184	tattcggtcgaccggaccatggccgacgacgacgtgct	25–50	tattcgccgcgggcaatagacccaggagaccgggac	2737–2760

			Real-time PCR primers and probe			
Gene name	**Accession no.**	**Sense primer**	**Sense primer position**	**Antisense primer**	**Antisense primer position**	**Probe**	**Probe position**
SynCAM1	AF539424	ccctcctcccacaacaacc	1033-1051	ggtcccctcttcacctgctc	1107–1126	cacctccatccttaccatcatcacagattct	1075–1105

were processed for easier user analysis using the INTERACT interface (16). Once this information was obtained, single ion chromatograms were reconstructed for each peptide pair using XPRESS software (13).

Plasmid constructs

For promoter assays, we used a DNA fragment containing 1.9 kb from the 5′ flanking region of the human *SynCAM1* gene (NM_014333). The DNA fragment was isolated by PCR and cloned into the pGL3 vector (Promega, Madison, WI). The fragment extends to 50 bp upstream from the ATG translation initiation site in exon 1. The sense and antisense primers used for amplification are listed in Table 1; the primer positions are relative to the human chromosome 11 genomic contig (NT_033899). ErbB4 receptors were expressed using expression plasmids encoding either the full-length human erbB4 (herbB4) (17), or a mutated form of erbB4 (DNerbB4), lacking the intracellular domain of the receptor (7). To generate a DN SynCAM1 expression plasmid we used a 1.2-kb DNA fragment extending from the transcription start site through the transmembrane domain of mouse SynCAM1 (mSynCAM1). The latter includes the cell membrane targeting domain of the mSynCAM1 isoform 4 gene (NM_018770). The DNA fragment was isolated by PCR from an expression plasmid that contains the complete coding sequence of mSynCAM1 (18) and using primers listed in Table 1. The amplified product was directional cloned using *Bgl*II and *Sal*I into pEGFP-N1 (Promega) and is referred to as pEGFP-N1 DN SynCAM1. To generate the construct that targets DN Syn-CAM1 to astrocytes we digested pEGFP-N1 DN SynCAM1 with *Eco*RI and *Not*I and blunt-ligated the fragment into the pGfa2-Lac1 backbone (19), thus placing DN SynCAM1 under control of the human GFAP promoter. This plasmid is referred to as pGFAP DN SynCAM1. To generate the calcium/calmodulin-dependent serine protein kinase (CASK) expression plasmid, we used a DNA fragment that encodes the complete coding sequence of the rat *CASK* gene (NM_022184). The DNA fragment used was isolated by PCR from a pEGFP-CASK expression plasmid (generously donated by Dr. Thomas Südhof, Stanford University, School of Medicine, Palo Alto, CA), using primers listed in Table 1. The CASK PCR product was then directional cloned using *Sal*I and *Sac*II into pDsRed2-N1 (Promega).

Yeast two-hybrid assay

Two-hybrid assays were performed using the yeast strain EGY48 harboring LacZ and LEU2 reporters, as described (20).

The erbB4 intracellular domain (amino acid residues 676-1308) (21) was generated by PCR, subcloned into *Not*I/*Eag*I sites of pEG202, and used as bait. The intracellular domain of Syn-CAM1 (18) and PSD-95 PDZ domains 1 and 2 (a gift from Dan Pak and Morgan Sheng, Massachusetts Institute of Technology, Boston, MA) were subcloned into the *Eco*RI/*Xho*I site of pJG4–5. Oligonucleotide-directed PCR mutagenesis was used to create the mutant (K751M) kinase-dead erbB4 receptor. All constructs were verified by DNA sequencing.

DN SynCAM1 transgenic mice

After removing the DN SynCAM1 construct from the pGfa2-Lac1 backbone by digestion with *Eco*R1, the GFAP DN Syn-CAM1 transgene was injected into the pronucleus of FvB/N1 zygotes. DN SynCAM1 positive offspring were identified by PCR genotyping with primers that specifically amplify a region spanning the junction between the SynCAM1 and enhanced green fluorescence protein (EGFP) coding regions of the transgene (Table 1). The following PCR conditions were used for genotyping: an initial activation step of 5 min at 95 C, followed by 39 cycles of denaturing at 95 C for 30 sec, annealing at 55 C for 30 sec, and extension at 72 C for 1 min, and a final extension at 72 C for 10 min. The samples were loaded onto a 2% agarose gel and the PCR products were visualized by ethidium bromide staining.

The tissue distribution of the DN SynCAM1 protein in transgenic mice was characterized by Western blotting, and its cellular distribution in brain by immunohistofluorescence. To determine the effect of the DN SynCAM1 transgene on reproductive biology, we conducted several experiments. Litters consisting of WT and heterozygous DN SynCAM1 mice from both line (L) 27 and L45 were weaned on d 18, and the females were placed in groups of five per cage. Starting on d 21, the animals were inspected daily for vaginal opening. The time of first ovulation was functionally confirmed by mating WT and DN SynCAM1 females at the age of vaginal opening with WT males and determining the time interval between mating and delivery of a litter for each group. The day of mating was determined by confirming the presence of a copulatory plug in the mouse's vagina; this day was considered as d 0 of pregnancy. When litters were born, the date and number of pups were recorded. Average litter size, interval between vaginal opening and first ovulation, and interval between vaginal opening and birth of the first litter were calculated. The females were bred for two consecutive litters, and L45 females were subsequently used for assessment of estrous cyclicity. To perform this experiment, the animals were left undisturbed after weaning

the second litter; at 4–6 months of age, vaginal lavages were performed daily for 3 wk, and the different phases of their estrous cycle were recorded.

Statistical analysis

Quantitative data were analyzed using SigmaStat 3.1 software (Systat Software Inc., San Jose, CA). The data were first subjected to a normality test and an equal variance test. Data that passed these two tests were then analyzed as follows: comparison of two groups was performed with the Student's t test, data sets containing more than two groups were analyzed with one-way ANOVA followed by the Student-Newman-Keuls multiple test for individual means. Data that failed either the normality or equal variance test were analyzed by nonparametric methods such as the Mann-Whitney rank sum test (two groups), the Kruskal-Wallis one-way ANOVA on ranks followed by the Student-Newman-Keuls method of pair-wise multiple comparison procedure (multiple groups). The null hypothesis was rejected at the 0.05 level for all analyses.

Supplemental material and methods

A detailed description of procedures involving cell culture, antibodies, Western blots, immunoprecipitation assays, immunohistofluorescence, RNA extraction, real-time PCR, promoter assays, PGE_2, and GnRH assays is provided as Supplementary Material and Methods (published on The Endocrine Society's Journals Online web site at http://end.endojournals.org).

Results

Quantitative proteomic analysis reveals a reduction in SynCAM1 levels in the hypothalamus of mice with disrupted astrocytic erbB receptor signaling

Because in rodents most GnRH neurons are located in the POA of the hypothalamus, we collected this region from reproductively immature 28-d-old WT and GFAP-DNerbB4 female mice and subjected it to tandem mass spectrometry-ICAT analysis. The most reproducible finding (five independent hits) was a decrease in the levels of SynCAM1 in transgenics (Fig. 1, A–C). Western blot analysis of the POA using a monoclonal antibody (3E1) that specifically recognizes SynCAM1 (22) confirmed this reduction (Fig. 1, D and E). Polyclonal antibodies (18, 22) (pleio-SynCAM antibodies) that recognize the protein products from three of the four known SynCAM genes (*SynCAM1, -2,* and *-3*) (22) showed that the mouse hypothalamus also contains SynCAM2 and -3 but that the abundance of these proteins does not change in the mutant animals (not shown).

SynCAM1 abundance in astrocytes is regulated by erbB4 signaling

SynCAM1, an adhesion protein expressed in neurons (18) and some glial populations (23), has been implicated

in the formation and organization of excitatory synapses in brain (18, 22). Because the mechanisms regulating SynCAM1 expression and function are not understood, it was intriguing that SynCAM1 expression in the hypothalamus was reduced as a consequence of disrupted astrocytic erbB receptor signaling. Therefore, we sought to examine the possibility that alterations in SynCAM1 levels in the hypothalamus of GFAP-DNerbB4 mice reflects, at least in part, changes in astrocytic SynCAM1 expression. Levels of SynCAM1 protein were compared in cultures of astrocytes purified from WT and transgenic mice. Western blot analysis using the SynCAM1 antibody 3E1 (Fig. 2, A and B) revealed that the abundance of SynCAM1 was strikingly reduced in astrocytes from GFAP-DNerbB4 mice. Furthermore, treatment of WT hypothalamic astrocytes with NRGβ1 (3 nM) significantly ($P <$ 0.05) increased SynCAM1 mRNA levels (Fig. 2C) and SynCAM1 protein levels (Fig. 2D). These results indicate that NRGβ1-erbB signaling promotes SynCAM1 expression in astrocytes.

To determine whether the effects of NRG1-erbB signaling on SynCAM1 expression are mediated by transcriptional mechanisms, we used a luciferase reporter assay. A 1.9-kb DNA fragment containing the 5′ flanking region of the human *SynCAM1* gene was cloned into a luciferase reporter plasmid. This construct was then transfected into the astrocytic progenitor cell line BAS-8.1 (24), which does not express erbB4 receptors (data not shown). Treatment of BAS-8.1 cells with NRGβ1 (3 nM) did not change the activity of the SynCAM1 reporter construct. However, when an erbB4-expression plasmid was cotransfected with the luciferase reporter plasmid, NRGβ1 treatment increased SynCAM1 promoter activity by 2-fold ($P <$ 0.01) (Fig. 2E). Importantly, transient expression of DNerbB4 did not affect basal SynCAM1 promoter activity but obliterated the stimulatory effect of NRGβ1 on cells expressing the full-length receptor (Fig. 2E). These results indicate that activation of astrocytic erbB4 receptor contributes to maintaining glial synthesis of SynCAM1 via transactivation of SynCAM1 gene transcription.

Ligand-dependent activation of astrocytic erbB4 receptors results in physical association of the receptors with SynCAM1

In addition to mediating cell adhesion via its extracellular domain, SynCAM1 uses specific motifs of its intracellular domain to interact with other membrane-associated proteins and initiate signal transduction (11, 18). Considering these findings, we sought to determine whether SynCAM1 can physically interact with erbB4 receptors. First, we compared the cellular distribution of
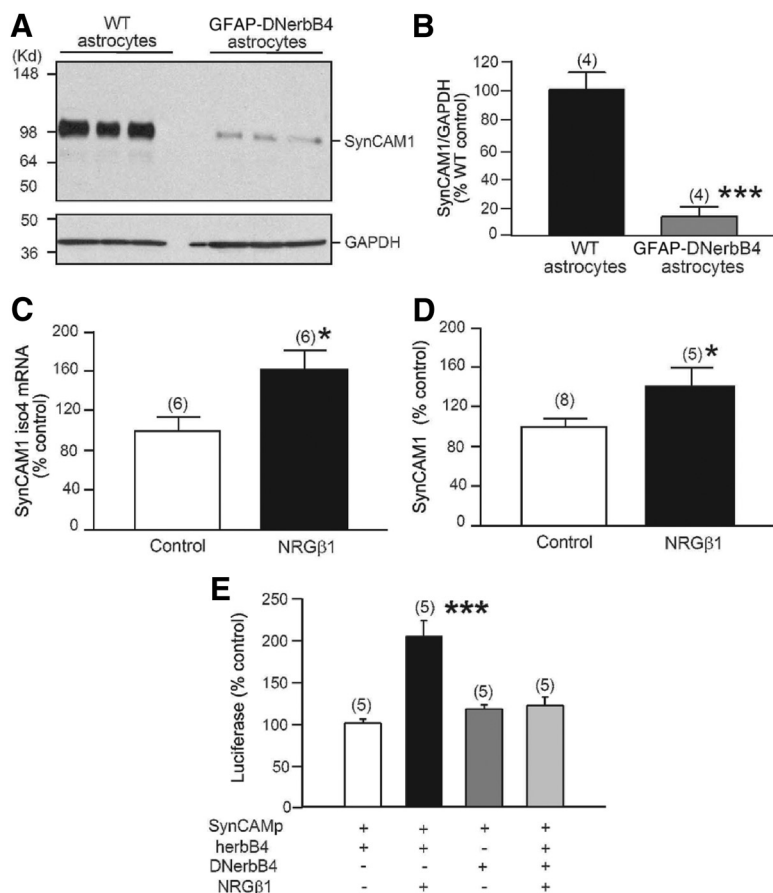
FIG. 1. The abundance of SynCAM1 is reduced in the POA of immature mice with disrupted astrocytic erbB4 receptor signaling (GFAP-DNerbB4), as assessed by ICAT-μLC-MS/MS and Western blot. Peptides from the POA of WT and GFAP-DNerbB4 mice were labeled with the light and heavy form of the ICAT reagent, respectively. A, A representative mass chromatogram of the sequencing of one of the SynCAM1 peptide pairs detected using tandem mass spectrometry. The selected peptides were fragmented using CID, and the resultant C-terminus (b_3, y_1) and N-terminus (b_1, y_3) ions are displayed. B, Reconstructed single ion chromatograms of the isotopically light (WT) and heavy (GFAP-DNerbB4) SynCAM1 peptide partners, created by plotting the intensity of the signal observed at the relevant m/z value (light, 1138.405; heavy 1141.093) as a function of retention time (minutes). The area under the curve fitted to the SynCAM1 peptide ions pairs was greatly reduced in the GFAP-DNerbB4 samples compared with wild-type (WT: 5.00E+07; GFAP-DNerbB4: 1.57E+07). The *numbers in the upper right-hand corner* represent the scale of each chromatogram. C, Heavy to light ratio of five SynCAM1 peptides sequenced from WT (light) and GFAP-DNerbB4 (heavy) samples (measured by the area under the curve on the chromatogram using the INTERACT software package) shows erbB4-dependent SynCAM1 expression. **, $P < 0.02$ *vs.* WT animals. D, Decreased SynCAM1 protein levels in the POA of 30-d-old female GFAP-DNerbB4 mice as determined by Western blot analysis using antibody 3E1 (25 μg of protein per lane). E, Densitometric analysis of the SynCAM1 signal shown in D. **, $P < 0.02$ *vs.* WT animals. *Numbers in parentheses above bars* represent the number of independent observations per group, and *vertical lines* are SEM.

erbB4 and SynCAM immunoreactivity in hypothalamic astrocytes stimulated with NRGβ1 (3 nM). In nonstimulated cells, erbB4 immunoreactivity (*red*) was diffuse and not associated with SynCAM (*green*, Fig. 3, A and C). Forty minutes after NRGβ1 administration, erbB4 receptors appear to cluster on the cell membrane, as suggested

FIG. 2. erbB4 receptors are required to maintain SynCAM1 expression in hypothalamic astrocytes. A, SynCAM1 protein levels are decreased in GFAP-DNerbB4 hypothalamic astrocytes in culture. Protein extracts were probed with SynCAM1 monoclonal antibody 3E1 and anti-glyceraldehyde-3-phosphate dehydrogenase (GAPDH) antibodies. B, Densitometric analysis of blot shown in A. ***, $P < 0.01$ *vs.* WT astrocytes. C, SynCAM1-isoform 4 mRNA levels in hypothalamic astrocytes assessed by real-time RT-PCR increases 8 h after stimulating erbB4 receptors with NRGβ1 (3 nM). *, $P < 0.05$. D, SynCAM1 protein levels increased in hypothalamic astrocytes after 16 h of NRGβ1 treatment. *, $P < 0.05$. E, NRGβ1 (3 nM, 8 h) increases SynCAM1 promoter activity in BAS 8.1 astrocyte progenitor cells transiently expressing human erbB4 (herb4) receptors, and this effect is abolished by overexpression of a DNerbB4 receptor. ***, $P < 0.01$ *vs.* all other groups. *Numbers in parentheses above bars are* number of independent observations per group, and *vertical lines* are SEM.

by the presence of punctate staining (*red*, Fig. 3, B and D); many of these erbB4 clusters appeared to be associated with regions of SynCAM localization. This apparent association was particularly conspicuous in astrocytic processes (nonstimulated controls in Fig. 3C *vs.* NRGβ1-treated cultures in Fig. 3D).

The distribution patterns of erbB4 and SynCAM1 after NRG1 treatment suggested that these proteins become physically associated after activation of erbB4 receptors. To test this possibility, we performed coimmunoprecipitation studies. Although SynCAM1-erbB4 interactions could not be detected in unstimulated astrocytes, coimmunoprecipitation was observed after a brief (10 min) stimulation with NRGβ1 (1 nM) (Fig. 3E), suggesting that ligand-induced erbB4 activation prompts this receptor to associate with SynCAM1. Because we and others have

shown that the intracellular domain of erbB4 (E4ICD) can bind to certain intracellular proteins after it is activated (4, 25), we used a yeast two-hybrid assay to test whether E4ICD is capable of directly interacting with the intracellular domain of SynCAM1 (Fig. 3F). The results showed that WT active E4ICD interacts with SynCAM1 intracellular domain, and this interaction is abolished when E4ICD activity is eliminated by a point mutation in tyrosine 751 (K751M) (4). Thus, upon exposure to NRGβ1, erbB4 and SynCAM1 associate directly through their intracellular domains.

Astrocyte-specific disruption of SynCAM1 intracellular domain inhibits SynCAM1 intracellular interactions

The ability of SynCAM1 to interact with erbB4 via its intracellular domain raised the possibility that SynCAM1 may use its intracellular domain to elicit signaling events needed for astrocytes to stimulate GnRH release. To address this issue, we generated transgenic mice carrying a DN SynCAM1 under the transcriptional control of the human GFAP promoter to target expression of the transgene to astrocytes. The DN SynCAM1 transgene has intact extracellular and transmembrane domains but lack the intracellular protein 4.1, ezrin, radixin, moesin (FERM) and PDZ [postsynaptic density protein (PSD95); Drosophila disc large tumor suppressor (DlgA), and zonula occludens-1 protein (zo-1)] domains, which are replaced with a sequence encoding EGFP (Fig. 4A). Theoretically, the DN SynCAM1 protein should adhere to endogenous SynCAM proteins both *in cis* and *in trans* via the extracellular IgG domains but would antagonize signaling events mediated by the intracellular FERM and PDZ domains (11, 18). Live-cell imaging of BAS 8.1 cells transfected with DN SynCAM1 demonstrated that the mutant protein was appropriately targeted to the plasma membrane (Fig. 4, C and D), compared with a diffuse, cytoplasmic localization seen in cells transfected with a cytomegalovirus plasmid eGFP-N1 expression vector (Fig. 4B). The distribution of DN SynCAM1 also closely resembles the distribution of endogenous SynCAM in hypothalamic astrocytes (12).
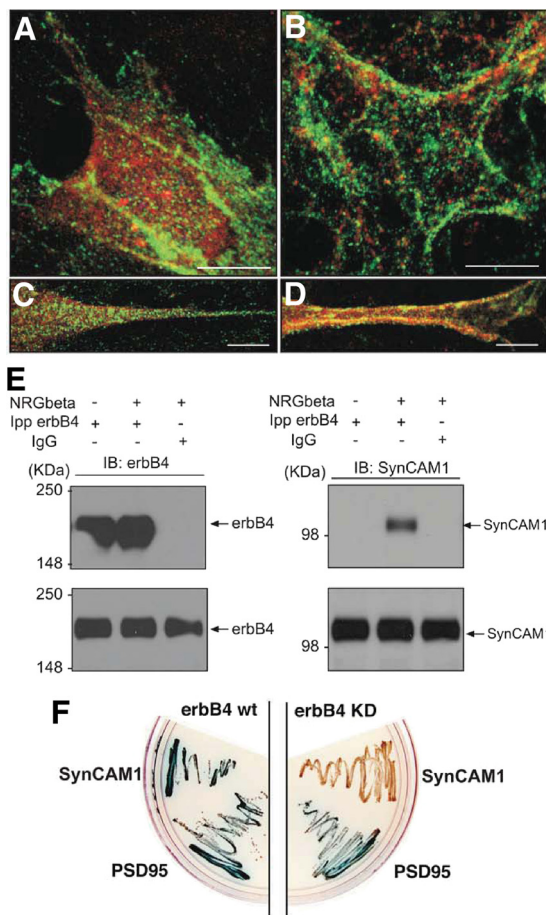
FIG. 3. Ligand-dependent activation of erbB4 receptors induces a direct SynCAM1-erbB4 receptor association in hypothalamic astrocytes. A–D, Overlaid confocal images of SynCAM (*green*) and erbB4 (*red*) immunoreactivity in WT astrocytes. A and B, Cell bodies of nonstimulated (A) and NRGβ1-treated (3 nM, 45 min) WT astrocytes (B). C and D, Zoomed confocal overlaid images of cell processes from nonstimulated (C) and NRGβ1- treated astrocytes (D). E, Stimulation of erbB4 receptors with NRGβ1 (1 nM, 10 min) causes interaction between erbB4 and SynCAM1. Proteins from astrocytes either left unstimulated (lane 1) or stimulated with NRGβ1 (lane 2) were immunoprecipitated (Ipp) with an agarose-coupled erbB4 antibody and blotted for SynCAM1 (*upper right panel*). Controls for the immunoprecipitation include blotting the precipitates with erbB4 antibody (*upper left panel*) and immunoprecipitation with IgG. Correct blotting was confirmed by probing nonprecipitated cell lysates (5% input) for erbB4 and SynCAM1 (*lower right* and *left panels*, respectively). F, Targeted yeast two-hybrid assay using the SynCAM1 intracellular domain as pray and the erbB4 intracellular domain as bait. WT-erbB4, but not an erbB4 receptor carrying an inactivating point mutation of the kinase domain (erbB4 KD), interacts with SynCAM1 (expression of LacZ, *blue color*). PSD95, which interacts with the C-terminal PDZ binding motif of erbB4 but not with SynCAM1, served as a positive control. *Bars* (B–E), 10 μm.

To determine whether DN SynCAM1 acts in a dominant-negative fashion, we first assessed the ability of the transgene to interact with WT SynCAM1. Human embryonic kidney 293T cells transfected with expression vectors encoding WT SynCAM1 and DN SynCAM1 showed colocalization of both proteins at the cell membrane (Fig. 5, A–C), suggesting a physical association between the two
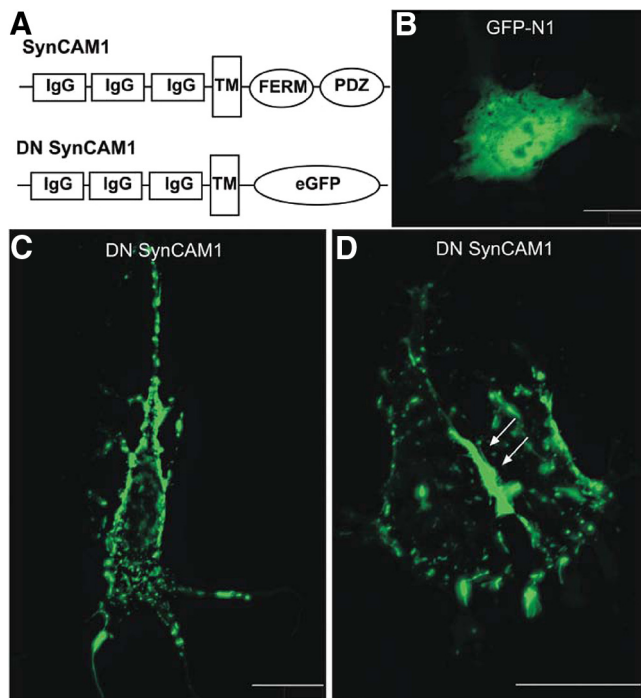

FIG. 4. DN SynCAM1 protein is targeted to the plasma membrane of live astrocytes in culture. A, Schematic illustration of the WT and DN SynCAM1 proteins. DN SynCAM1 contains the complete extracellular, transmembrane, and cell membrane targeting domains of WT SynCAM1 but lacks the intracellular domain. Instead this domain is replaced by a sequence encoding EGFP. B, Live cell image of an immortalized BAS8.1 cultured astrocyte transfected with the positive control cytomegalovirus plasmid eGFP-N1 expression plasmid. C and D, Live cell images of BAS8.1 cultured astrocytes transfected with the DN SynCAM1 expression plasmid. Note that eGFP-N1 is diffusely present throughout the cytoplasm (B), whereas DN SynCAM1 is targeted to the cell membrane (C). Also notice the accumulation of DN SynCAM1 protein at points of cell to cell adhesion (D, *arrows*). *Bars* (B and C), 20 μm; (D), 25 μm.

proteins. Coimmunoprecipitation of WT SynCAM1 by antibodies to the EGFP moiety of DN SynCAM1 verified this interaction (Fig. 5D). Next, we assessed the ability of the transgene to disrupt the known interaction of SynCAM1 with the scaffold protein CASK, and the resulting recruitment of this protein from the cytosol to the cell membrane (18). Consistent with earlier findings (18), a CASK-red fluorescent protein (RFP) fusion protein expressed in 293T cells exhibited a diffuse cytoplasmic distribution (Fig. 6A, *left panels*), but when the cells were also transfected with an expression vector encoding WT SynCAM1, CASK was recruited to the cell membrane (Fig. 6A, *left middle panels*). As expected, DN SynCAM1 alone did not affect the cytoplasmic distribution of CASK (Fig. 6A, *right middle panels*); however, it did block CASK recruitment to the cell membrane by WT SynCAM1 (Fig. 6A, *right panels*). CASK immunoprecipitation resulted in the coprecipitation of SynCAM1, an interaction that was prevented by DN SynCAM1 (Fig. 6B). These results indicate that DN SynCAM1 acts as a dominant-negative mol-
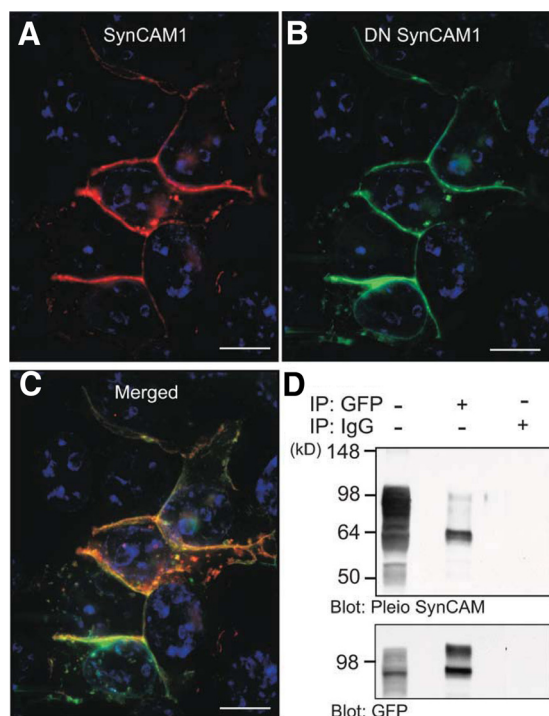
FIG. 5. DN SynCAM1 directly interacts with SynCAM1 in transfected 293T cells. A and B, A single confocal section of 293T cells transfected with expression plasmids encoding WT SynCAM1 (A, *red*) and DN SynCAM1 (B, *green*) shows that both proteins are localized to the plasma membrane. C, Merged image suggests that SynCAM1 and DN SynCAM colocalize at the plasma membrane. D, Coimmunoprecipitation assay of protein extracts from 293T cells transfected with SynCAM1 and DN SynCAM1 confirm that the proteins are physically associated. SynCAM1 and DN SynCAM1 interaction was identified in protein extracts that were immunoprecipitated with EGFP antibodies then blotted with Pleio SynCAM antibodies (*upper membrane*). To confirm the pulldown of DN SynCAM1 in the immunoprecipitation, the membrane was stripped and reprobed with EGFP antibodies (*lower membrane*). Lane 1 was loaded with 100 μg of protein extract from 293T cells transfected with SynCAM1 and DN SynCAM1 that was not immunoprecipitated before Western blot analysis. Lane 3 is a negative control in which the cell proteins were immunoprecipitated using the IgG fraction of rabbit serum in lieu of EGFP antibodies. *Bars* (A–C), 10 μm. Cell nuclei in A–C (*blue color*) are stained with Hoechst nuclear stain.

ecule able to prevent SynCAM1 intracellular domain-mediated interactions.

Astrocyte-specific disruption of SynCAM1 function delays female sexual development and adult reproductive function

Using the DN SynCAM1 construct, we generated transgenic mice and selected two lines (L27 and L45) for further study. We assessed transgene expression by Western blots using antibodies against green fluorescent protein (GFP) for DN SynCAM1 detection and proteins extracted from brain (cerebral cortex and hypothalamus) and several peripheral tissues (heart, lung, liver, spleen, kidney, adrenal, and ovary). Although no GFP-immunoreactive proteins were detected in any tissues from WT mice (Fig. 7A), the

cerebral cortex and hypothalamus of both L45 (Fig. 7B) and L27 (data not shown) transgenic mice showed a protein of a size similar to that expected for the DN SynCAM1 transgene. No such protein was detected in peripheral tissues, indicating that DN SynCAM1 expression is confined to the nervous system. At the cellular level, no GFP immunohistofluorescence was detected in astrocytes from WT animals (Fig. 7C), but astrocytes for DN SynCAM1 mice exhibited an abundance of the DN SynCAM1 protein (Fig. 7D, *green color*). As previously shown for astrocytes identified in the transgenic Brainbow mouse (26), the GFP immunoreactive material was distributed beyond the area of GFAP staining, likely reflecting the presence of DN SynCAM1 in astrocytic processes not stained for GFAP. No DN SynCAM1 was detected in neurons identified by the presence of the neuronal marker HUC/D (Fig. 7, E–G). In fact, DN SynCAM1 astrocytes appear to be in intimate contact with neuronal cell bodies, as evidenced by regions amid the astrocytes that are completely devoid of DN SynCAM1 labeling (Fig. 7E, *arrows*), but contain neuronal cell bodies (Fig. 7, F and G, *red*).

Female mice from both L27 and L45 lines displayed a delay in age at vaginal opening (Fig. 8A) and first estrous (Fig. 8B) compared with WT littermates. Because both L27 and L45 show identical patterns of DN SynCAM1 expression and a similar delay in reproductive maturation, we used L27 mice to assess the animals' fecundity and L45 mice to evaluate alterations in estrous cyclicity. The DN SynCAM1 mice had a trend toward a reduced number of pups in the first litter and an even greater and significant reduction in litter sizes in the second and subsequent litters compared with WT dams (Fig. 8C). The estrous cycle was also disrupted in DN SynCAM1 mice (Fig. 8, D and E). The mutant animals had a significant decrease in the incidence of proestrous (when the preovulatory surge of gonadotropins occurs) and a corresponding increase in the incidence of estrous (Fig. 8D). Examples of estrous cycles from two WT and two mutant animals across a 21-d period illustrate this alteration in cyclicity (Fig. 8E).

Disrupting SynCAM1 in astrocytes impairs neuregulin-stimulated release of PGE$_2$ and GnRH

The above-described reproductive deficits are similar to those previously seen in mice with defective astrocyte erbB4 function (7). Considering that NRGβ1 stimulates GnRH secretion indirectly by eliciting PGE$_2$ release from astrocytes (7), we investigated the possibility that the ability of NRGβ1 to stimulate GnRH release is compromised in DN SynCAM1 mice. Hypothalamic astrocytes from WT astrocytes respond to NRGβ1 (3 nM, 16 h) with PGE$_2$ release, but astrocytes from DN SynCAM1 mice fail to do so (Fig. 8F). To determine whether this deficiency also
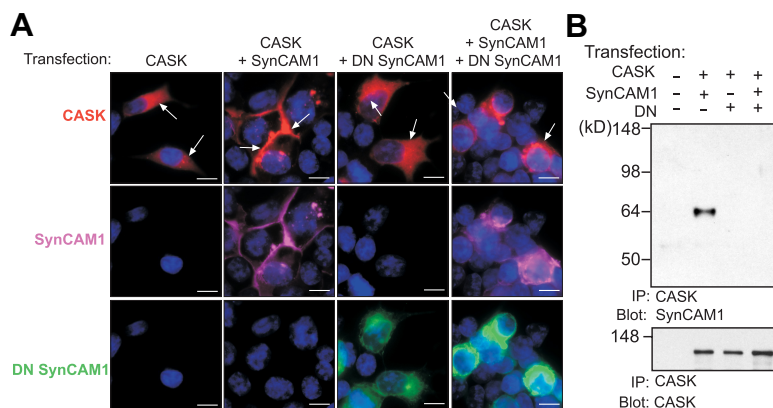
FIG. 6. DN SynCAM1 inhibits SynCAM1 function by preventing SynCAM1 association to, and the cellular redistribution of, the scaffold, actin-binding protein CASK. A, *left panels*, Human embryonic kidney 293T cells transfected with a CASK-RFP expression plasmid show a cytoplasmic CASK localization (*red*). *Left middle panels*, Cotransfection of CASK-RFP with WT SynCAM1 results in CASK recruitment to the plasma membrane were SynCAM1 is localized (*purple*). *Right middle panels*, Cotransfection of DN SynCAM1 with CASK-RFP does not affect the cytoplasmic localization of the CASK protein (*red*), despite the presence of DN SynCAM1 (*green*) at the plasma membrane. *Right panel*, DN SynCAM1 prevents the SynCAM1-dependent recruitment of CASK-RFP to the plasma membrane. B, DN SynCAM1 prevents the association of WT SynCAM1 to CASK-RFP as assessed by coimmunoprecipitation assay of protein extracts from 293T cells transfected with CASK-RFP, WT SynCAM1, and DN SynCAM1. The proteins were immunoprecipitated with CASK antibodies and blotted with SynCAM1 monoclonal antibodies. To confirm CASK pulldown, the membrane was reprobed with CASK antibodies (*lower panel* in B). Bars, 10 μm. Cell nuclei (*blue*) are stained with Hoechst.

occurs in an *in vivo* context, median eminence (ME) explants from WT and DN SynCAM1 mice were exposed to NRGβ1 (3 nM, 1 h), and the incubation medium was assayed for GnRH. The ME of DN SynCAM1 mice had a lower ($P < 0.05$) basal GnRH secretion compared with the WT control. Furthermore, the ME from WT mice, but not that from DN SynCAM1 mutants, responded to NRGβ1 with GnRH release (Fig. 8G). Despite this difference, the DN SynCAM1 and WT ME explants released comparable levels of GnRH following K$^+$ stimulation (Fig. 8H). These findings indicate that DN SynCAM1 mice have an impaired astrocytic PGE$_2$ response to neuregulins. They also suggest that this deficit decreases the ability of erbB receptor activation to stimulate GnRH release from GnRH nerve terminals.

Discussion

SynCAM1 is a member of the Ig superfamily, a large group of proteins involved in cell surface recognition (27, 28). In vertebrates, four SynCAM genes, sharing highly conserved intracellular and extracellular domains have been described (11). SynCAM1 is abundant in brain neurons in which it functions as a synaptic adhesion molecule that promotes synaptic assembly (18) and enhances excitatory synaptic transmission (22, 29). In a companion paper (12), we show that, consistent with its known neuronal site of expression, Syn-CAM1 is conspicuous in GnRH neurons, but in addition it

is abundantly expressed in hypothalamic astrocytes. In the present report, we show that astrocytic SynCAM1 contributes to the process by which astroglial cells regulate female reproductive capacity. Syn-CAM1 associates with erbB4 receptors via its intracellular domain. Interfering with this association compromises the ability of hypothalamic astrocytes to respond to erbB4 receptor activation with PGE$_2$ release and to elicit GnRH release from the ME of the hypothalamus. The physiological importance of these Syn-CAM1 intracellular actions is underscored by the distinct reproductive phenotype of delayed puberty, disrupted estrous cyclicity, and reduced fecundity observed in transgenic mice that have a disruption in endogenous astrocytic Syn-CAM1 function.

Loss of SynCAM1 function in astrocytes delayed, but did not prevent puberty. This outcome is similar to the results of previous studies dealing with molecules that are involved in the control of puberty, but do not play a central role in the process. For instance, mice carrying a dominant-negative form of erbB4 targeted to astrocytes have a delayed first ovulation, but exhibit normal adult reproductive capacity (7). Additional examples are mice carrying a point mutation of the erbB1 receptor (30, 31) and mice lacking the Janus-activated kinase 2 in GnRH neurons (32) or lacking the homeodomain protein Six6 also in GnRH neurons (33). The most tenable explanation for the absence of complete infertility resulting from these deficiencies is the existence of redundant and compensatory circuits that become operative when one system fails to perform. In the present situation, the compensatory activation of additional adhesive molecules with signaling capabilities in the astrocyte-GnRH neuron interface, such as the neuronal contactin/glial receptor-like protein tyrosine phosphatase-β system (34), may contribute to explaining the delayed puberty and the partial loss of fertility observed in DN SynCAM1 mice.

SynCAM1 was earlier proposed to be a member of a regulatory gene network that operates in the hypothalamus to control female reproductive competence (35, 36). This notion was initially supported by the observation of increased SynCAM1 mRNA expression in the hypothalamus of peripubertal monkeys as compared with juvenile animals (35). The finding that SynCAM1 mediates astrocyte-to-astrocyte and astrocyte-GnRH neuron communication (12), demonstrates that SynCAM1 is indeed an in-
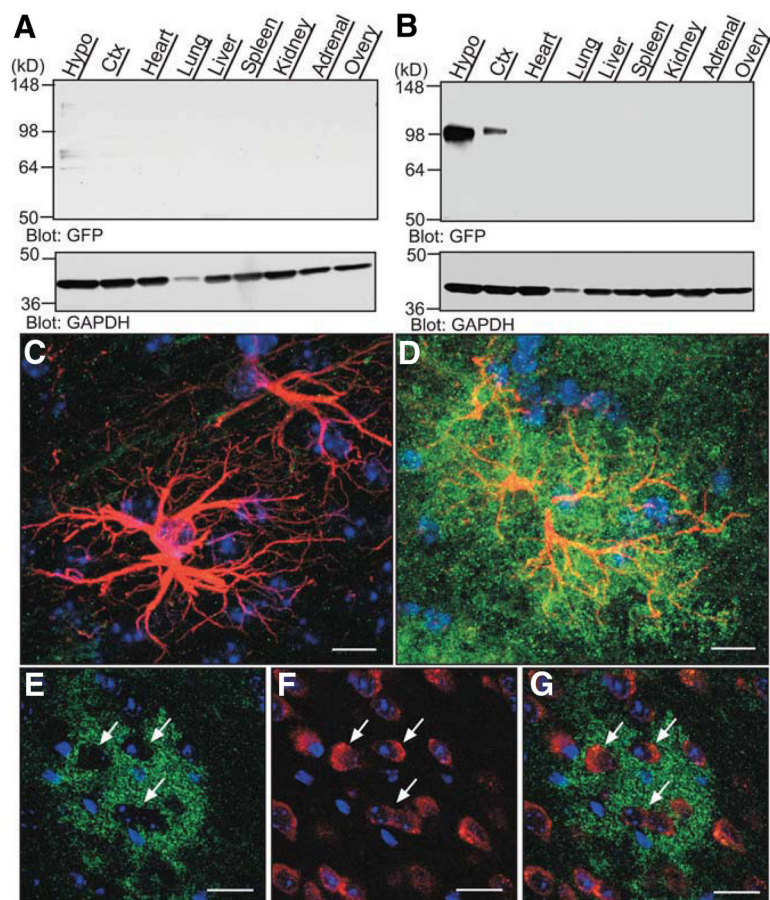
FIG. 7. DN SynCAM1 is selectively expressed in astrocytes within the adult female hypothalamus. A, DN SynCAM1 protein, detected with GFP antibodies, is absent in WT tissues. B, DN SynCAM1 protein expression is confined to the central nervous system in transgenic mice. Ctx, Cerebral cortex; Hypo, hypothalamus. C–G, DN SynCAM1 immunoreactivity is confined to astrocytes in the transgenic mouse brain. C, Merged confocal projection images showing the absence of DN SynCAM1 immunostaining (GFP antibodies, *green*) in WT hypothalamic astrocytes identified with antibodies to GFAP (*red*). D, DN SynCAM1 is abundant in hypothalamic astrocytes from a DN SynCAM1 animal. E–G, DN SynCAM1 is not expressed in neurons. E, Single confocal section showing DN SynCAM1 immunoreactivity (*green*) associated with cellular structures surrounding immunonegative cells (identified by Hoechst staining of cell nuclei). F, Immunostaining of neurons using HUC/D antibodies (*red*). G, Merged image of single confocal sections showing that HUC/D immunoreactive cells are devoid of DN SynCAM1 protein. Bars (C and D), 20 μm; (E–G), 40 μm. Cell nuclei (*blue*) are stained with Hoechst.

tegral component of neuroendocrine reproductive function. In the present study, we show that the abundance of SynCAM1 in WT astrocytes is maintained through signaling events initiated by erbB4 and that SynCAM1 expression is depressed in hypothalamic astrocytes from GFAP-DNerbB4 mice. Binding of NRGβ1 to erbB4 receptors leads, to enhanced SynCAM1 gene expression by directly transactivating the SynCAM1 promoter. Although NRGs are recognized by both erbB3 and erbB4 receptors (2), the latter appear to be the only type of erbB receptor involved in regulating astroglial SynCAM1 expression or function under *in vivo* conditions because neither hypothalamic nor cerebrocortical astrocytes express erbB3 receptors (5).

It has been recognized for some time that adhesion molecules, such as E-cadherin, carcinoembryonic antigen-related cell adhesion molecule 1, and neural cell adhesion molecule, can modify the effect of growth factors, such as basic fibroblast growth factor and epidermal growth factor, on cell function (37–40). However, the converse, *i.e.* the ability of growth factor receptor activation to influence the function of adhesion molecules, has not been examined. Our results provide evidence for this concept. Under basal conditions, erbB4 and SynCAM1 do not appear to be associated, but this independence terminates rapidly after the receptor is exposed to NRGβ1. The present results also demonstrate that activated erbB4 receptors and SynCAM1 interact via their intracellular domains. This is in contrast to the behavior of neural cell adhesion molecule, which engages basic fibroblast growth factor receptors via its extracellular domain (41). How the intracellular SynCAM1 sequences associate with activated erbB4 receptors remains to be defined.

Like many other adhesion molecules of the immunoglobulin superfamily (28), SynCAM1 is capable of signal transduction. It is endowed with an intracellular domain containing both a FERM binding motif and a C-terminus sequence recognized by proteins containing PDZ domains type II (11, 42). Binding of membrane associated proteins (such as protein 4.1, CASK, and syntenin) to the FERM- and PDZ-domain binding sequences, link SynCAM1 to signaling events resulting in the structural reorganization of the cytoskeleton (42, 43). Our sEM studies (12) indicate that the initial, adhesive cell response to SynCAM1 involves cytoskeletal reorganization. We observed that GnRH neuronal processes, formed within minutes of presenting SynCAM1-Fc coated beads to the cells, trap the beads via SynCAM1-SynCAM1 homophilic interactions.

Our results do not identify the cellular mechanisms underlying the ability of DN SynCAM1 to disrupt astrocytic SynCAM1 intracellular function. Several possibilities can be considered based on known SynCAM functions. For instance, SynCAM1 has been shown to selectively enhance excitatory neurotransmission (29) and work in concert
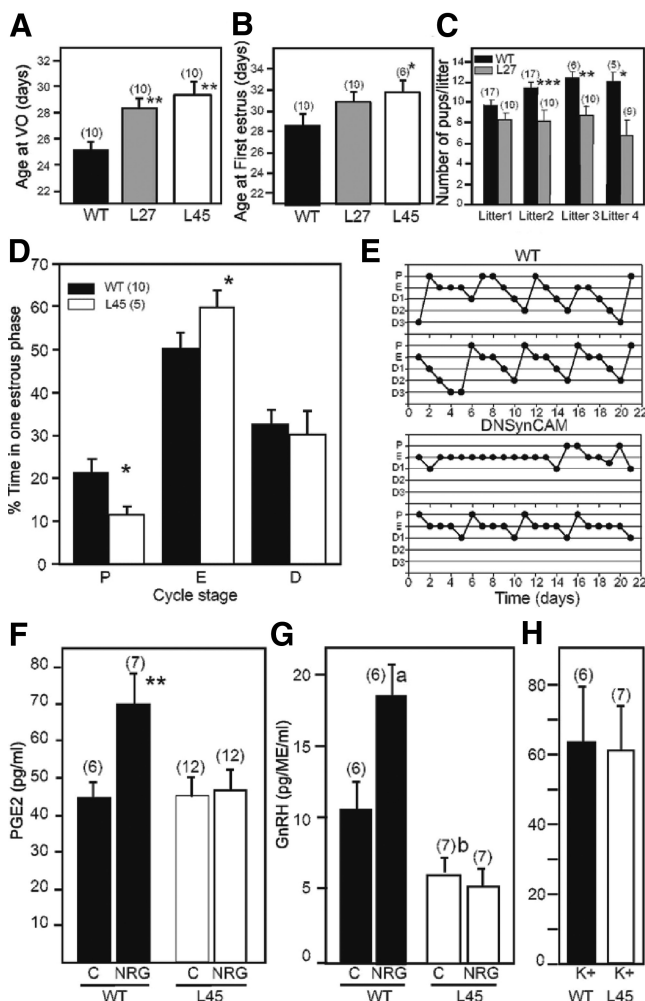
required for normal reproductive development (45, 46). Therefore, it is tempting to speculate that astroglial SynCAM1 may act as an adhesion/signaling molecule able to organize excitatory neuron-to-glia signaling domains in hypothalamic astrocytes.

Complementing this view are our immunohistofluorescence results showing that SynCAM molecules cluster in both astrocytes and neurons as a consequence of erbB4 receptor activation. Such clustering suggests the formation of hot spots of cell adhesion and signaling domains. SynCAM1 interactions with downstream effectors may contribute to both cytoskeletal reorganization and receptor distribution. One potential downstream effector may be CASK because homophilic SynCAM1 interactions recruit CASK to the cell membrane (18), and we show here that overexpression of DN SynCAM1 abolishes this redistribution. CASK plays a role in both actin reorganization and receptor distribution. Through interactions with syndecan-4 and protein 4.1, CASK is coupled to both the Rho signaling pathway, involved in mediating reorganization of the cytoskeleton (47) and the actin cytoskeleton (48, 49). CASK has also been shown to sort *N*-methyl-D-aspartate receptors (50) and serve as binding partner to glutamate receptor interacting protein (51). In *Caenorhabditis elegans*, Lin2, a CASK ortholog, is associated with epidermal growth factor receptor targeting (52). It remains to be determined whether similar interactions also occur in astrocytes.

CASK has also been shown to interact with the N and P/Q type of voltage-gated calcium channels in neurons (53,

FIG. 8. Transgenic targeting of DN SynCAM1 to astrocytes disrupts reproductive development and adult reproductive function in female mice. Panels A–E, Female DN SynCAM1 transgenic mice have deficits in reproductive development and mature reproductive function capacity. Panel A, Delayed vaginal opening. Panel B, Delay in the age at first estrus. Panel C, Reduced female fecundity assessed by the number of pups per litter delivered by each dam. Panel D, Irregular estrous cycle. Panel E, Examples of estrous cycles tracked for 21 d in two WT (*upper panels*) and two DN SynCAM1 (*lower panels*) mice. Panels F–H, DN SynCAM1 mice have diminished astrocyte and GnRH neuron responsiveness to NRG stimulation. Panel F, Cultured WT hypothalamic astrocytes, but not astrocytes from DN SynCAM1 mice, respond to NRGβ1 (3 nM, 16 h) stimulation with increased PGE$_2$ secretion. C, Control, basal PGE$_2$ levels before exposure to NRGβ1. Panel G, ME explants from DN SynCAM1 mice have lower basal GnRH and fail to release GnRH in response to NRGβ1 (3 nM, 2 h). Panel H, ME explants from WT and DN SynCAM1 mice release comparable levels of GnRH after K$^+$ stimulation. *Numbers in parentheses* are number of animals or cultures per group. *Bars* represent means and *vertical lines* are the mean ± SEM. *, $P < 0.05$ and **, $P < 0.02$ *vs.* WT controls; a, $P < 0.02$ and b, $P < 0.05$ *vs.* basal GnRH levels in WT controls.

with glutamatergic receptors to generate functional excitatory synaptic contacts (18, 29). One mechanism by which SynCAM1 regulates excitatory neurotransmission is through the recruitment of *N*-methyl-D-aspartate or 2-amino-3-hydroxy-5-methyl-4-isoxazol propionic acid receptors via the intracellular FERM binding domain of SynCAM1 (44). Hypothalamic astrocytes express both metabotropic glutamate and 2-amino-3-hydroxy-5-methyl-4-isoxazol propionic acid receptors, which upon activation initiate a signaling cascade that leads to erbB receptor activation and glia-to-neuron signaling events

54). If similar interactions occurred in astrocytes, SynCAM1 may not only regulate astroglial plasticity but may also be involved in facilitating two well-established components of astrocyte physiology: calcium influx and release of excitatory neurotransmitters. The impact of these alterations at the whole-animal level is anticipated to be noticeable, a premise supported by the distinct alterations in reproductive function we observed in DN SynCAM1 transgenic mice, which appear to be even more severe than those seen in DNerbB4 animals (7). DN SynCAM1 mice

exhibited not only delayed puberty (assessed by the age at vaginal opening and first estrus) but also a disruption of reproductive cyclicity in addition to reduced fecundity (evidenced by the smaller size of litters born to the mutant mice in comparison with WT controls).

In summary, the present study unveils a physiological role for SynCAM1-mediated intracellular signaling in the process by which astrocytes of the neuroendocrine brain control female sexual development and mature reproductive function. Our results demonstrate a functional connection between glial erbB4 receptors and SynCAM1. We show that ligand-dependent erbB4 receptor activation results in physical association of the receptor to SynCAM1 via their intracellular domains. In addition, SynCAM1 synthesis is increased. Disruption of astrocytic SynCAM1 signaling via a dominant negative SynCAM1 form disrupts the ability of neuregulin to stimulate PGE$_2$ formation in astrocytes and to release GnRH from the hypothalamus, implicating SynCAM1 as a mediator of erbB4 activation in hypothalamic astrocytes. The consequences of this interaction are evidenced by the finding that mice with disrupted astrocytic SynCAM1 signaling have delayed puberty and reduced reproductive capacity in adulthood. Our findings raise the possibility of similar erbB4 receptor-SynCAM1 interactions mediating glia-to-neuron communication in brain regions other than the hypothalamus.

Acknowledgments

References

1. Holbro T, Hynes NE 2004 ErbB receptors: directing key signaling networks throughout life. Annu Rev Pharmacol Toxicol 44:195–217
2. Buonanno A, Fischbach GD 2001 Neuregulin and ErbB receptor signaling pathways in the nervous system. Curr Opin Neurobiol 11:287–296
3. Adlkofer K, Lai C 2000 Role of neuregulins in glial cell development. Glia 29:104–111
4. Sardi SP, Murtie J, Koirala S, Patten BA, Corfas G 2006 Presenilin-dependent ErbB4 nuclear signaling regulates the timing of astrogenesis in the developing brain. Cell 127:185–197
5. Ma YJ, Hill DF, Creswick KE, Costa ME, Cornea A, Lioubin MN, Plowman GD, Ojeda SR 1999 Neuregulins signaling via a glial erbB2/erbB4 receptor complex contribute to the neuroendocrine control of mammalian sexual development. J Neurosci 19:9913–9927
6. Rage F, Lee BJ, Ma YJ, Ojeda SR 1997 Estradiol enhances prostaglandin E$_2$ receptor gene expression in luteinizing hormone-releasing hormone (LHRH) neurons and facilitates the LHRH response to PGE$_2$ by activating a glia-to-neuron signaling pathway. J Neurosci 17:9145–9156
7. Prevot V, Rio C, Cho GJ, Lomniczi A, Heger S, Neville CM, Rosenthal NA, Ojeda SR, Corfas G 2003 Normal female sexual development requires neuregulin-erbB receptor signaling in hypothalamic astrocytes. J Neurosci 23:230–239
8. Gygi SP, Rist B, Gerber SA, Turecek F, Gelb MH, Aebersold R 1999 Quantitative analysis of complex protein mixtures using isotope-coded affinity tags. Nat Biotechnol 17:994–999
9. Aebersold R, Goodlett DR 2001 Mass spectrometry in proteomics. Chem Rev 101:269–295
10. Tao WA, Aebersold R 2003 Advances in quantitative proteomics via stable isotope tagging and mass spectrometry. Curr Opin Biotechnol 14:110–118
11. Biederer T 2006 Bioinformatic characterization of the SynCAM family of immunoglobulin-like domain-containing adhesion molecules. Genomics 87:139–150
12. Sandau US, Mungenast AE, McCarthy J, Biederer T, Corfas G, Ojeda SR 2011 The synaptic cell adhesion molecule, SynCAM1, mediates astrocyte-to-astrocyte and astrocyte-to-GnRH neuron adhesiveness in the mouse hypothalamus. Endocrinology:2353–2363
13. Ranish JA, Yi EC, Leslie DM, Purvine SO, Goodlett DR, Eng J, Aebersold R 2003 The study of macromolecular complexes by quantitative proteomics. Nat Genet 33:349–355
14. Yi EC, Lee H, Aebersold R, Goodlett DR 2003 A microcapillary trap cartridge-microcapillary high-performance liquid chromatography electrospray ionization emitter device capable of peptide tandem mass spectrometry at the attomole level on an ion trap mass spec-

trometer with automated routine operation. Rapid Commun Mass Spectrom 17:2093–2098

15. **Eng JK, McCormack AL, Yates III JR** 1994 An approach to correlate tandem mass spectral data of peptides with amino acid sequences in a protein database. J Am Soc Mass Spectrom 5:976–989

16. **Han DK, Eng J, Zhou H, Aebersold R** 2001 Quantitative profiling of differentiation-induced microsomal proteins using isotope-coded affinity tags and mass spectrometry. Nat Biotechnol 19:946–951

17. **Elenius K, Corfas G, Paul S, Choi CJ, Rio C, Plowman GD, Klagsbrun M** 1997 A novel juxtamembrane domain isoform of HER4/erbB4. J Biol Chem 272:26761–26768

18. **Biederer T, Sara Y, Mozhayeva M, Atasoy D, Liu X, Kavalali ET, Südhof TC** 2002 SynCAM, a synaptic adhesion molecule that drives synapse assembly. Science 297:1525–1531

19. **Brenner M, Kisseberth WC, Su Y, Besnard F, Messing A** 1994 GFAP promoter directs asotrycte-specific expression in transgenic mice. J Neurosci 14:1030–1037

20. **Finley Jr RL, Thomas BJ, Zipursky SL, Brent R** 1996 Isolation of Drosophila cyclin D, a protein expressed in the morphogenetic furrow before entry into S phase. Proc Natl Acad Sci USA 93:3011–3015

21. **Plowman GD, Culouscou JM, Whitney GS, Green JM, Carlton GW, Foy L, Neubauer MG, Shoyab M** 1993 Ligand-specific activation of HER4/p180^{erbB4}, a fourth member of the epidermal growth factor receptor family. Proc Natl Acad Sci USA 90:1746–1750

22. **Fogel AI, Akins MR, Krupp AJ, Stagi M, Stein V, Biederer T** 2007 SynCAMs organize nascent synapses through heterophilic adhesion. J Neurosci 27:12516–12530

23. **Thomas LA, Akins MR, Biederer T** 2008 Expression and adhesion profiles of SynCAM molecules indicate distinct neuronal functions. J Comp Neurol 510:47–67

24. **Bongarzone ER, Foster LM, Byravan S, Verity AN, Landry CF, Schonmann VV, Amur-Umarjee S, Campagnoni AT** 1996 Conditionally immortalized neural cell lines: potential models for the study of neural cell function. Methods 10:489–500

25. **Carpenter G** 2003 ErbB-4: mechanism of action and biology. Exp Cell Res 284:66–77

26. **Livet J, Weissman TA, Kang H, Draft RW, Lu J, Bennis RA, Sanes JR, Lichtman JW** 2007 Transgenic strategies for combinatorial expression of fluorescent proteins in the nervous system. Nature 450:56–62

27. **Williams AF, Barclay AN** 1988 The immunoglobulin superfamily—domains for cell surface recognition. Annu Rev Immunol 6:381–405

28. **Rougon G, Hobert O** 2003 New insights into the diversity and function of neuronal immunoglobulin superfamily molecules. Annu Rev Neurosci 26:207–238

29. **Sara Y, Biederer T, Atasoy D, Chubykin A, Mozhayeva MG, Südhof TC, Kavalali ET** 2005 Selective capability of SynCAM and neuroligin for functional synapse assembly. J Neurosci 25:260–270

30. **Prevot V, Lomniczi A, Corfas G, Ojeda SR** 2005 ErbB-1 and erbB-4 receptors act in concert to facilitate both female sexual development and mature reproductive function. Endocrinology 146:1465–1472

31. **Apostolakis EM, Garai J, Lohmann JE, Clark JH, O'Malley BW** 2000 Epidermal growth factor activates reproductive behavior independent of ovarian steroids in female rodents. Mol Endocrinol 14:1086–1098

32. **Wu S, Divall S, Hoffman GE, Le WW, Wagner KU, Wolfe A** 2011 Jak2 is necessary for neuroendocrine control of female reproduction. J Neurosci 31:184–192

33. **Larder R, Clark DD, Miller NL, Mellon PL** 2011 Hypothalamic dysregulation and infertility in mice lacking the homeodomain protein six6. J Neurosci 31:426–438

34. **Parent AS, Mungenast AE, Lomniczi A, Sandau US, Peles E, Bosch MA, Rønnekleiv OK, Ojeda SR** 2007 A contactin-receptor-like protein tyrosine phosphatase β complex mediates adhesive communication between astroglial cells and gonadotrophin-releasing hormone neurones. J Neuroendocrinol 19:847–859

35. **Roth CL, Mastronardi C, Lomniczi A, Wright H, Cabrera R, Mungenast AE, Heger S, Jung H, Dubay C, Ojeda SR** 2007 Expression of a tumor-related gene network increases in the mammalian hypothalamus at the time of female puberty. Endocrinology 148:5147–5161

36. **Ojeda SR, Lomniczi A, Mastronardi C, Heger S, Roth C, Parent AS, Matagne V, Mungenast AE** 2006 Minireview: the neuroendocrine regulation of puberty: is the time ripe for a systems biology approach? Endocrinology 147:1166–1174

37. **Povlsen GK, Berezin V, Bock E** 2008 Neural cell adhesion molecule-180-mediated homophilic binding induces epidermal growth factor receptor (EGFR) down-regulation and uncouples the inhibitory function of EGFR in neurite outgrowth. J Neurochem 104:624–639

38. **Abou-Rjaily GA, Lee SJ, May D, Al-Share QY, Deangelis AM, Ruch RJ, Neumaier M, Kalthoff H, Lin SH, Najjar SM** 2004 CEACAM1 modulates epidermal growth factor receptor-mediated cell proliferation. J Clin Invest 114:944–952

39. **Andl CD, Rustgi AK** 2005 No one-way street: cross-talk between e-cadherin and receptor tyrosine kinase (RTK) signaling: a mechanism to regulate RTK activity. Cancer Biol Ther 4:28–31

40. **Hintermann E, Yang N, O'Sullivan D, Higgins JM, Quaranta V** 2005 Integrin α6β4-erbB2 complex inhibits haptotaxis by up-regulating E-cadherin cell-cell junctions in keratinocytes. J Biol Chem 280:8004–8015

41. **Kiselyov VV, Skladchikova G, Hinsby AM, Jensen PH, Kulahin N, Soroka V, Pedersen N, Tsetlin V, Poulsen FM, Berezin V, Bock E** 2003 Structural basis for a direct interaction between FGFR1 and NCAM and evidence for a regulatory role of ATP. Structure 11:691–701

42. **Hung AY, Sheng M** 2002 PDZ domains: structural modules for protein complex assembly. J Biol Chem 277:5699–5702

43. **Hoover KB, Bryant PJ** 2000 The genetics of the protein 4.1 family: organizers of the membrane and cytoskeleton. Curr Opin Cell Biol 12:229–234

44. **Hoy JL, Constable JR, Vicini S, Fu Z, Washbourne P** 2009 SynCAM1 recruits NMDA receptors via protein 4.1B. Mol Cell Neurosci 42:466–483

45. **Dziedzic B, Prevot V, Lomniczi A, Jung H, Cornea A, Ojeda SR** 2003 Neuron-to-glia signaling mediated by excitatory amino acid receptors regulates erbB receptor function in astroglial cells of the neuroendocrine brain. J Neurosci 23:915–926

46. **Lomniczi A, Cornea A, Costa ME, Ojeda SR** 2006 Hypothalamic tumor necrosis factor-α converting enzyme (TACE) mediates excitatory amino acid-dependent neuron-to-glia signaling in the neuroendocrine brain. J Neurosci 26:51–62

47. **Hall A** 2005 Rho GTPases and the control of cell behaviour. Biochem Soc Trans 33:891–895

48. **Bass MD, Humphries MJ** 2002 Cytoplasmic interactions of syndecan-4 orchestrate adhesion receptor and growth factor receptor signalling. Biochem J 368:1–15

49. **Biederer T, Sudhof TC** 2001 CASK and protein 4.1 support F-actin nucleation on neurexins. J Biol Chem 276:47869–47876

50. **Jeyifous O, Waites CL, Specht CG, Fujisawa S, Schubert M, Lin EI, Marshall J, Aoki C, de Silva T, Montgomery JM, Garner CC, Green WN** 2009 SAP97 and CASK mediate sorting of NMDA receptors through a previously unknown secretory pathway. Nat Neurosci 12:1011–1019

51. **Hong CJ, Hsueh YP** 2006 CASK associates with glutamate receptor interacting protein and signaling molecules. Biochem Biophys Res Commun 351:771–776

52. **Kaech SM, Whitfield CW, Kim SK** 1998 The LIN-2/LIN-7/LIN-10 complex mediates basolateral membrane localization of the C. elegans EGF receptor LET-23 in vulval epithelial cells. Cell 94:761–771

53. **Maximov A, Südhof TC, Bezprozvanny I** 1999 Association of neuronal calcium channels with modular adaptor proteins. J Biol Chem 274:24453–24456

54. **Maximov A, Bezprozvanny I** 2002 Synaptic targeting of N-type calcium channels in hippocampal neurons. J Neurosci 22:6939–6952